


Evaluating the Scope of Malignant Bone Tumor Using ADC Measurement on ADC Map

Technology in Cancer Research & Treatment
 Volume XX: 1-6
 © The Author(s) 2019
 Article reuse guidelines:
sagepub.com/journals-permissions
 DOI: 10.1177/1533033819853267
journals.sagepub.com/home/tct


Haisong Chen, MD, PhD¹ , Zengjie Wu, MD¹,
 Wenjian Xu, MD, PhD¹ , Jing Pang, MD¹, Meng Jia, MD²,
 Cheng Dong, MD, PhD¹, and Xiaoli Li, MD¹

Abstract

Background: It is very important for surgeons to know the accurate borders of malignant bone tumors before they can precisely resect the tumors. The objective of the study is to investigate the usefulness of apparent diffusion coefficient value for estimating the extent of malignant bone tumor. **Methods:** VX2 tumor fragments were implanted into the tibiae of 30 rabbits. After 4 weeks, magnetic resonance plain scans were performed and then tumor specimens were cut into sagittal sections and partitioned into histology slices for dot-to-dot comparisons with microscopic findings. The sizes of the tumors measured separately on specimen, conventional magnetic resonance imaging sequences, and diffusion-weighted imaging (by measuring apparent diffusion coefficient value on apparent diffusion coefficient mapping) were compared statistically with each other. **Results:** The mean tumor sizes measured on specimen and apparent diffusion coefficient mapping (by calculating apparent diffusion coefficient value) were 5.20 ± 0.89 cm and 5.31 ± 0.87 cm, respectively; there was no significant difference between the 2 ($P > .05$). The tumor sizes measured on T1WI, T2WI, T2WI with fat suppression were 4.82 ± 0.87 cm, 5.58 ± 0.87 cm, 5.63 ± 0.85 cm, respectively, and these values were significantly different from that measured on specimen (5.20 ± 0.89 cm, $P < .05$). **Conclusion:** The extent of the VX2 malignant bone tumor can be estimated accurately by measurement of apparent diffusion coefficient value.

Keywords

diffusion magnetic resonance imaging, neoplasms, bone tissue, rabbits, ADC

Abbreviations

ADC, apparent diffusion coefficient; CT, computed tomography; DWI, diffusion-weighted imaging; MRI, magnetic resonance imaging.

Received: January 20, 2018; Revised: March 21, 2019; Accepted: April 24, 2019.

Introduction

It is very important for surgeons to know the accurate borders of malignant bone tumors before they can precisely resect the tumors.¹ In our previous study, we had used the computed tomography (CT) spectral curves to discriminate between the microinfiltration and simple edema zones,² but the curves are indirect to show the extent of lesions. Therefore, further studies are needed to directly and accurately display the tumor zones. Magnetic resonance imaging (MRI) is useful for determining the extent of tumors depended on signal intensities.³ However, conventional MRI is limited in providing satisfactory information on tumor extent because of the difficulty displaying microinvasion and the interference of edema.⁴ Hence, new imaging approaches are needed to accurately determine the extent of malignant bone tumors.⁵

In the present study, we evaluated findings of diffusion-weighted imaging (DWI), a kind of functional MRI, in a rabbit VX2 tumor model to explore whether apparent diffusion coefficient (ADC) value measurement on ADC map can accurately determine the extent of the tumor.

¹ Department of Radiology, The Affiliated Hospital of Qingdao University, Qingdao, China

² Department of Ultrasound, The Women and Children's Hospital of Qingdao, Qingdao, China

Corresponding Author:

Wenjian Xu, MD, PhD, Department of Radiology, The Affiliated Hospital of Qingdao University, Qingdao 266003, China.
 Email: 1021540101@qq.com



Methods and Materials

Subjects

The rabbit VX2 carcinoma models were established as described in our previous study.² A total of 30 healthy New Zealand white rabbits were used. Of all, 1.6 mL/kg ketamine and 1 mL/kg diazepam were injected into the muscles of the rabbits before any operations were performed.

Animal Model

The tumor-bearing rabbits were provided by the animal laboratory of our hospital. The VX2 tumor fragments were cut from the tumor in the thigh of a tumor-bearing rabbit with a scalpel and implanted into the proximal part of right tibiae of healthy rabbits using an electrical drill and forceps. Then the bone defect was sealed with wax and then the muscle and skin at the site of incision were sutured.

Magnetic Resonance Methods

Four weeks after the tumor implantation, MRI was performed on anesthetized animals in the supine position with a 3.0 T MR imager (Sigma, General Electric Healthcare, Milwaukee, Wisconsin) using a human knee coil. All images were obtained in the sagittal plane. In all sequences, the field of view was 100 mm × 100 mm, matrix size 192 × 256, slice thickness 2 mm, and intersection gap was 1 mm. Magnetic resonance imaging with sequences of DWI (TR = 4000 milliseconds, TE = 75 milliseconds, b factor = 0, and 1000 s/mm²), T1WI (TR = 500 milliseconds, TE = 10 milliseconds), T2WI (TR = 2000 milliseconds, TE = 100 milliseconds), and T2WI with fat suppression was performed. The bandwidth of the DWI sequence was 83.3 kHz. After MR scanning, ADC mappings of the whole tibiae with tumors were automatically formed.

Pathologic Examination

Air was injected into the ear veins of unconscious rabbits to kill them after MR examinations and then the rabbits were preserved in a refrigerator at a temperature of -50°C. After completely frozen, the calves of rabbits were cross-sectioned into sagittal slices with a thickness of 2 mm (Figure 1), and the central section was selected to match the corresponding MR image. Then, the sample was cut into blocks with an edge length of 2 cm to match the size of the glass slide. The tissue dot got from the specimen can be found its location in the MR image with the same coordinate value by the square grids as in Figure 2. Tissue sections were numbered for dot to dot comparison with MR images. Then the samples were dipped in 10% formalin (fixation), and 4% nitric acid (decalcification), embedded in paraffin blocks, sectioned, and stained using hematoxylin and eosin.



Figure 1. Maximal sagittal section of the specimen of rabbit calves with a slice thickness of 2 mm.

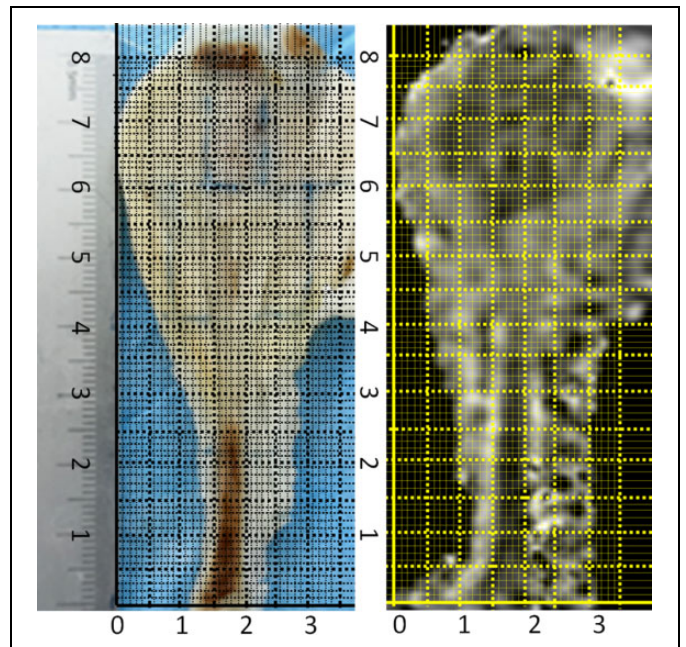


Figure 2. The square grids in the 2 figures form a coordinate system respectively that permits a dot-to-dot comparison by identical coordinate value. The tissue dot got from the specimen can be found its location in the MR image (ADC map) with the same coordinate value. ADC indicates apparent diffusion coefficient; MR, magnetic resonance.

Analysis of Pathological and MR Findings

Histopathologic presentations were evaluated by 2 pathologists under consensus regarding the border of tumor on sagittal section of specimen by dot-to-dot comparisons with microscopic findings of pathologic slices.



Figure 3. Magnetic resonance image of T2WI corresponding to the specimen of Figure 1.



Figure 4. Maximal sagittal sections of magnetic resonance image of T1WI.

Magnetic resonance images were assessed by 2 radiologists in consensus with respect to the border of the tumor on the above MR images including T2WI (Figure 3), T1WI (Figure 4), T2WI with fat suppression (Figure 5), and DWI-ADC mapping (Figure 6). The radiologists performing measurements were blinded to pathology results.

The margin of tumor on T1WI, T2WI, and T2WI with fat suppression was based on differences of signal intensity. The



Figure 5. The size of the tumor was measured on maximal sagittal sections of MR T2WI with fat suppression (the perpendicular line parallels to the front margin of the tibial cortex, and horizontal line is perpendicular to the above perpendicular line. The distance from A to B is the maximal anterior–posterior dimension of the tumor with the line AB parallel to the above horizontal line, and the distance from C to D is the maximal craniocaudal dimension of the tumor with the line CD parallel to the above perpendicular line). The signal of the tumor area (contoured by point A-D) is not very bright, possibly due to the relatively little water inside the rabbit VX2 tumor and the contrast with the surrounding edema. MR indicates magnetic resonance.

margin of tumor on DWI-ADC mapping depended on the differences of average ADC values rather than the differences of the signal intensity based on b-value images.

The transition area between the solid tumor and the normal zone is consisted of microinfiltration area and edema. The microinfiltration area is defined as the stretching region of a few tumor cells (Figure 7). The edema area means the pure edema region without any tumor cells inside it. The solid tumor is defined as areas inside the tumor without hemorrhage, necrosis, and cystic change. Normal tissue means the tissue without tumor cells or edema. The margin between the microinfiltration and the edema is regarded as the true margin of the tumor on histology and DWI. Even though there may be a few inflammatory cells inside the edema around the microinfiltration, these cells are arranged in a looser mode causing a higher ADC value than the infiltration area which is made of relatively tight tumor cells. There should be a sudden variation in ADC value between the edema (even though mixed with inflammatory cells) and the microinfiltration area.

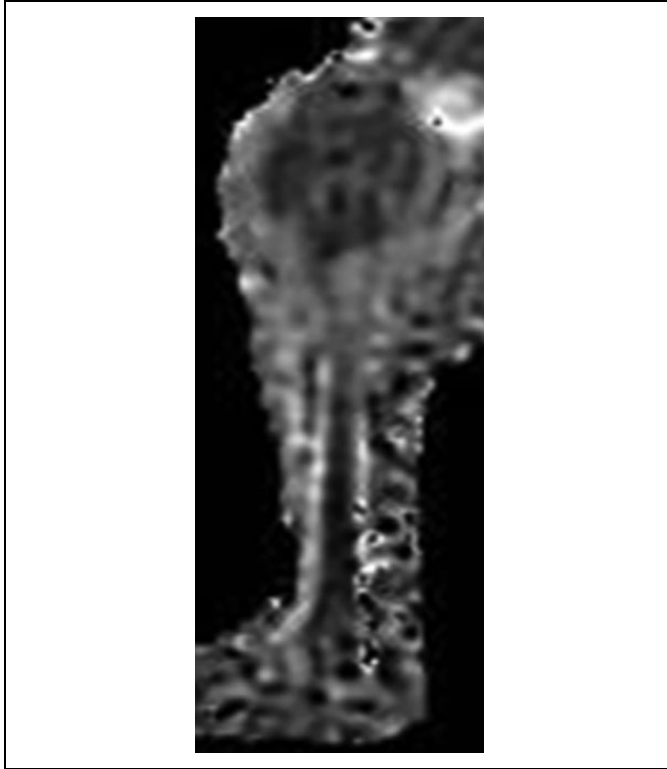


Figure 6. Maximal sagittal sections of MR image of ADC mapping. The margin of the tumor depended on the differences of ADC values rather than the differences of the signal intensity on the ADC mapping. ADC indicates apparent diffusion coefficient; MR, magnetic resonance.

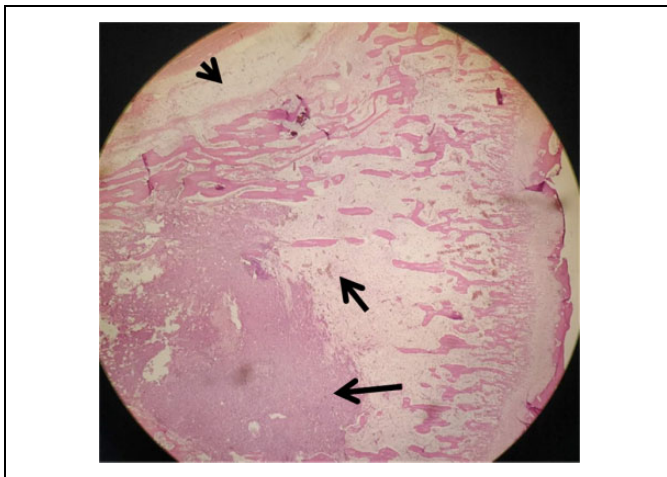


Figure 7. Pathological slice (hematoxylin-eosin stain, original magnification $\times 100$) displays tumor area (long arrow), microscopic tumor invasion area (short arrow), and bone marrow edema area (arrow head).

In our study, the ADC values were measured consecutively with Regions of Interest (ROI) sizes of 2 mm on ADC map. The ROIs were placed on the ADC map by one of the radiologists. The outer border with statistically different ADC values (which

were calculated automatically by a simple software designed for this study) between 2 sides was regarded as the margin of the tumor. The sizes of the tumors were measured separately on maximal sagittal sections of specimen and different MR images including DWI-ADC mapping, T1WI, T2WI, and T2WI with fat suppression. Because of the complexity to measure and calculate the maximal area of the irregular tumor on sagittal sections of specimen and MR images, we used the formula below to evaluate the size of tumor to simplify the study and reduce the numbers of variable parameters. The formula to calculate the size was the sum of maximal anterior–posterior and craniocaudal dimensions of the tumor (the perpendicular line paralleled to the front margin of the tibial cortex, and horizontal line was perpendicular to the above perpendicular line, Figures 5 and 6). Then the intercomparison of sizes was performed. Even though the anterior–posterior and craniocaudal dimensions could be analyzed separately, we didn't do this because that each of the 2 parameters could not reflex the size as a whole.

Statistical Analysis

All statistical calculations were performed with SPSS version 17.0 statistical software (IBM Corporation, Armonk, New York). All P values were 2 sided, and $P < .05$ was considered to indicate a statistically significant difference. Multiple comparisons with a statistical correction were first performed. If significant differences were found among the groups, then the paired t test was performed.

Approval regarding this study was obtained from the animal ethics committee of our hospital. The experiment complied with the Animal Research: Reporting of In Vivo Experiments (ARRIVE) guidelines and were carried out in accordance with the National Institutes of Health Guide for the Care and Use of Laboratory Animals (NIH Publications No. 8023, revised 1978).

Results

Successful modeling was achieved in all 30 rabbits, which was confirmed by histopathologic findings. The average ADC value of solid tumor, microinfiltration area, edema area, and normal tissue was 1.16 ± 0.06 , 1.45 ± 0.04 , 1.86 ± 0.06 , and 1.81 ± 0.05 , respectively. Multiple comparisons showed that there were significant differences among the groups, and the paired t test demonstrated that there was a significant difference of ADC value between every 2 regions of the former 3 (the solid tumor, microinfiltration, and edema area, $P < .05$), but there was no significant difference between the latter 2 (the edema and normal tissue, $P > .05$).

The mean tumor sizes measured on specimen and ADC mapping (by calculating ADC value) were 5.20 ± 0.89 cm and 5.31 ± 0.87 cm respectively, there was no significant difference between the 2 ($P > .05$). The tumor sizes measured on T1WI, T2WI, T2WI with fat suppression were 4.82 ± 0.87 cm, 5.58 ± 0.87 cm, 5.63 ± 0.85 cm, respectively, and these

values were significantly different from that measured on specimen (5.20 ± 0.89 cm, $P < .05$).

Discussion

The Border of VX2 Bone Tumor on Pathology

To accurately determine the border of osseous tumor preoperatively is vital to surgeons. Ahmad *et al*³ used the resected macroscopic tumor specimens as the gold standard for measuring the osseous extent of bone tumors. But the microinfiltration in the transition zone can't be found on gross specimens, and this may cause the underestimation of the tumor extent. The transition zone of bone tumor is the area between the tumor and the normal in regard to position and content, and it consists of few tumor cells (microinvasion) or/and edema (may be together with some inflammatory cells in case of necrosis).⁶ In the transition zone, the microinvasion part is the stretch of tumor zone, whose peripheral margin is the true border of the tumor, not disrupted by or mixed with edema or inflammatory cells.² Because of the transition area and different contents inside, the border of malignant bone tumor sometimes is difficult to be defined on medical imaging modalities such as conventional CT and MRI.

The Advantages and Disadvantages of Conventional MRI in the Evaluation of Malignant Bone Tumor Extension

Magnetic resonance was proved to be much more accurate than CT and radiography in the evaluation of intraosseous tumor length and soft tissue extension of musculoskeletal tumors.⁷ The good results of MR imaging are related to the superior contrast resolution.⁸ Furthermore, the MR images are not degraded by beam-hardening artifacts as are CT scans.⁹ All these make MR a good modality to evaluate the extent of malignant bone tumor. Despite this, the marrow edema in the vicinity of the tumor or in the transition area can influence the definition of tumor extent on the conventional MR images, and it is responsible for the overestimation of the tumor extent on T2WI with fat suppression and Short Time Inversion Recovery (STIR). As shown in the present study, the tumor size measured on T2WI with fat suppression was 5.63 ± 0.85 cm, which is larger than that measured on specimen under microscope (5.20 ± 0.89 cm, $P < .05$). So, many authors concluded that T1WI of MRI is unbiased at determining intraosseous tumor compared to STIR sequences or T2WI with fat suppression.^{3,10} But the transition zone including the microinfiltration of tumor may be easily overlooked on T1WI, causing the underestimation of the tumor range. As shown in the present study, the tumor size measured on T1WI was 4.82 ± 0.87 cm, that was smaller than that measured on specimen under microscope (5.20 ± 0.89 cm, $P < .05$). Functional MR, such as DWI or/and ADC map, is not found to study the border of bone tumor, even though it may provide more details of the information regarding the microinfiltration of the tumor in the transition area between the tumor and the normal part of the bone.

The Drawback of DW Images, ADC Mapping, and the Accuracy of ADC Measurement in Demonstrating the Extent of Malignant Bone Tumor

Diffusion-weighted imaging allows the assessment of the self-diffusion of water in biological tissues.¹¹ Diffusion-weighted imaging ADC mapping has been proven to be a sensitive modality to malignant tumors. Apparent diffusion coefficient maps are derived from multiple b-value images. At least 2 b values are required to calculate an ADC map.¹² In the present study, 2 b values of 0 and 1000 s/mm^2 are used. An ADC value in any tissue can be derived by drawing a region of interest on the ADC map. Diffusion-restricted tissue will have a lower ADC, whereas nonrestricted tissue will have a higher ADC. The relatively intensive tumor cells of microinfiltration in the transition zone restrict the motion of self-diffusion of water than that in the edema and reactive inflammatory area, causing the decreasing ADC, making it possible to display the true margin of the tumor. At first, we try to measure the tumor size on images of ADC map and compare with other MR sequences. But the inherent spatial resolution of ADC map is generally lower than the in-plane resolution of conventional MR imaging, making it impossible to distinguish the microinfiltration from the edema on ADC map with naked eyes, and DWI-ADC map is inherently prone to spatial distortion that could worsen size measurements in bone. So we used the differences of ADC value to contour the extent of the tumors. As shown in our study, the ADC value of microinfiltration area was 1.45 ± 0.04 , which was remarkably lower than that in edema area (1.86 ± 0.06 , $P < .05$). In the present study, the mean tumor sizes measured on VX2 tumor specimen (golden standard) and ADC mapping were 5.20 ± 0.89 cm and 5.31 ± 0.87 cm, respectively; no significant difference was found between the 2 ($P > .05$), indicating ADC map (by calculating ADC value) an accurate modality to demonstrate the border and extent of malignant bone tumor.

The Shortcomings of the Present Study

The present study had several limitations. First, although we proved in the present study that the range of the VX2 malignant bone tumor in a rabbit model could be estimated better by ADC measurement than other MR conventional sequences, it could not be absolutely true on human malignant bone tumors, for the primary bone tumors have a bony matrix, more or less pronounced, and one of the pitfall of DWI is the lowered sensitivity for sclerotic lesions which results in hypointensity or no changes of signal as well as ADC value on DWI and ADC mapping due to the lower or absent water content. Under this condition, CT images should be consulted to avoid underestimation of tumor extent. Second, ADC map is sensitive but may not specific for tumor invasion, there may be other factors besides tumor infiltration that could cause the decreasing ADC values,¹³ and further study is needed. Third, the formula to calculate the size (the sum of maximal transverse and perpendicular diameters of the tumor) is simple but may be

incomplete. It seems better to measure the area of tumor on maximal sagittal sections, even though the area is difficult to be calculated. Fourth, the spatial resolution explored here can be much higher than typically used in the clinic. This may mean that such methods for determining the infiltrative zone may not be applicable in the clinic unless a small Field of View (FOV) imaging approach is used. Fifth, the ROIs were placed on the ADC map by one of the radiologists, this could lead to bias when comparing ADC values between these regions. Finally, we included a small number of subjects (30 rabbits), and a larger sample is required for further evaluation.

Conclusion

The extent of the VX2 malignant bone tumor can be estimated accurately by measurement of ADC value.


Declaration of Conflicting Interests

The author(s) declared no potential conflicts of interest with respect to the research, authorship, and/or publication of this article.

Funding

The author(s) disclosed receipt of the following financial support for the research, authorship, and/or publication of this article: This work was supported by the National Natural Science Foundation of China under Grant 81571673, 81671658.

ORCID iD

Haisong Chen, MD, PhD  <https://orcid.org/0000-0002-4746-5193>
Wenjian Xu, MD, PhD  <https://orcid.org/0000-0002-1167-4866>

References

- Pozzi G, Albano D, Messina C, et al. Solid bone tumors of the spine: diagnostic performance of apparent diffusion coefficient measured using diffusion-weighted MRI using histology as a reference standard. *J Magn Reson Imaging*. 2017. doi:10.1002/jmri.25826. Epub ahead of print
- Chen H, Jia M, Xu W. Malignant bone tumor intramedullary Invasion: evaluation with dual-energy computed tomography in a rabbit model. *J Comput Assist Tomogr*. 2015;39(1):70-74.
- Ahmad S, Stevenson J, Mangham C, Cribb G, Cool P. Accuracy of magnetic resonance imaging in planning the osseous resection margins of bony tumors in proximal femur: based on corona T1-weighted versus STIR images. *Skeletal Radiol*. 2014;43(12):1679-1686.
- Rumpel H, Chong Y, Porter DA, Chan LL. Benign versus metastatic vertebral fractures: combined diffusion-weighted MRI and MR spectroscopy aids differentiation. *Eur Radiol*. 2013;23(2):541-550.
- Choi JA, Kang EY, Kim HK, Song IC, Kim YI, Kang HS. Evolution of VX2 carcinoma in rabbit tibia: magnetic resonance imaging with pathologic correlation. *Clin Imaging*. 2008;32(2):128-135.
- Bierry G, Venkatasamy A, Kremer S, Dosch JC, Dietemann JL. Dual-energy CT in vertebral compression fractures: performance of visual and quantitative analysis for bone marrow edema demonstration with comparison to MRI. *Skeletal Radiol*. 2014;43(4):485-492.
- Wang T, Wu X, Cui Y, Chu C, Ren G, Li W. Role of apparent diffusion coefficients with diffusion weighted magnetic resonance imaging in differentiating between benign and malignant bone tumors. *World J Surg Oncol*. 2014;12:365.
- Weber MA. MR Imaging of musculoskeletal tumors: what are new MR techniques capable of and what is included in an optimal MR protocol? *Radiologe*. 2013;53(5):396-398.
- Si MJ, Wang CS, Ding XY, et al. Differentiation of primary chordoma, giant cell tumor and schwannoma of the sacrum by CT and MRI. *Eur J Radiol*. 2013;82(12):2309-2315.
- Howe BM, Johnson GB, Wenger DE. Current concepts in MRI of focal and diffuse malignancy of bone marrow. *Semin Musculoskelet Radiol*. 2013;17(2):137-144.
- Subhawong TK, Jacobs MA, Fayad LM. Diffusion-weighted MR imaging for characterizing musculoskeletal lesions. *Radiographics*. 2014;34(5):1163-1177.
- Chavhan GB, Alsabban Z, Babyn PS. Diffusion-weighted imaging in pediatric body MR imaging: principles, technique, and emerging applications. *Radiographics*. 2014;34(3):E73-E88.
- Arkun R, Argin M. Pitfalls in MR imaging of musculoskeletal tumors. *Semin Musculoskelet Radiol*. 2014;18(1):63-78.